PERFORMANCE-BASED SEISMIC DESIGN OPTIMIZATION OF COMPOSITE MOMENT RESISTING FRAMES WITH CONCERET-FILLED STEEL COLUMNS AND STEEL BEAMS

H. Fazli[*, †]
Department of Civil Engineering, Payame Noor University, Tehran, Iran

ABSTRACT

In this paper, an optimization framework is developed for performance-based seismic design of composite moment frames consisting of concrete filled steel box columns and I-shaped steel beams. Material cost of the structure and seismic damage under severe earthquake ground motions are minimized as objective functions. Two design examples are presented to demonstrate the applicability and efficiency of the proposed method. Based on the obtained results, it is concluded that the proposed design optimization approach is capable of producing seismic designs of composite MRFs which are cost effective, provide reliable seismic performance and suffer less damage in the case of a severe earthquake ground motion.

Keywords: Optimization; Performance-based design; Seismic design; Composite structure; Colliding Bodies Optimization.

1. INTRODUCTION

Steel-concrete composite structures are becoming increasingly popular as an alternative to bare steel structures in moderate to high seismic zones, due to their efficiency and construction economy. Composite moment resisting frames as the most common lateral force resisting structures in the high seismic areas consist mainly of steel I girders and steel-concrete composite columns. The composite columns appear in two basic types, i.e. steel-encased concrete (SRC) where a structural steel shape is fully encased in reinforced concrete, and concrete filled steel tube (CFT) where an outer rectangular or circular tube is filled with concrete. CFT columns have several advantages over SRC columns because the

---

[*]Corresponding author:Department of Civil Engineering, Payame Noor University, Tehran, Iran
[†]E-mail address: hfazli@alumni.iust.ac.ir (H. Fazli)

steel tube serves as formwork and provides confinement to the concrete, thus eliminating the need for longitudinal and transverse reinforcement in the form of steel rebars. Additionally, the concrete infill helps to restrain local buckling from occurring in the wall of the steel tube.

Behavior and design of CFT composite structures has been the subject of extensive research studies in the last few decades. Significant information is made available through the studies on either component level behavior or overall structural performance. Experimental studies on behavior of CFT beam-columns are due to Tomii et al. [1], varma [2], ricles [3] and Roader [4]. CFT column-to-WF beam moment connections were studied by Chen [5], Choi [6] and Ricles [3]. Analytical studies have also been conducted to investigate the behavior of composite CFT components, for example Hajjar [7],Tort [8] and Denavit [9].

A number of researchers have focused on the overall seismic behavior of composite CFT moment resisting frames. Muhummud [10] investigated seismic behavior of special moment frames with CFT columns, steel wide flange beams and split-tee through-bolted connections, designed in accordance with code requirements. He concluded that frames designed in accordance with building code provisions for stiffness and strength, story drift limitations and strong column/weak-beam criterion satisfy Life Safety (LS) and Collapse Prevention (CP) performance levels under the Design Earthquake (DE) and Maximum Considered Earthquake (MCE) ground motion intensities, respectively.

Huang [11] investigated seismic behavior of moment resisting frames with high-strength square CFT columns. He employed analytical models with fiber-based elements and beam-column connection simulations. Based on the results of static pushover analyses, he concluded that high strength CFT MRFs meet the seismic performance objectives stipulated in current design codes.

Denavit et al. [12] investigated seismic performance factors for composite special moment frames. The moment frames consist of either CFT or SRC columns with split-tee connections and bolted flange plate connections, respectively. They concluded that composite frames possess high over-strength factors reflecting the drift-controlled design of these structures. Frames designed with $C_d=R$ (equal displacement rule) even have higher over-strength values due to increased estimated story drifts, that necessitate increased member sizes to satisfy the drift limits. Overall, the current seismic performance factors of $R=8$, $\Omega_0=3$ and $C_d=5.5$ are deemed satisfactory.

Another research by Hu et al. [13] also indicated that moment resisting CFT frames designed to satisfy the code limit 2% of magnified elastic inter-story drift ratio (ISDR) under design level earthquake loads, have acceptable performance under nonlinear static and dynamic analyses. The peak ISDRs obtained from nonlinear dynamic analyses satisfied the allowable design limit 2.5% with a fairly uniform distribution over the height of the structure as the number of stories increases. This indicates a conservative design of composite MRFs.

The above-mentioned research stream indicate that modern code provisions are relatively reliable in providing Life-Safe structural designs of CFT moment frames in zones of high-seismic hazard. However, using the insight provided by the aforementioned research, it is natural to ask for a more general design philosophy that enables designers and owners to select higher performance levels in order to limit property and business interruption losses

while looking for more cost effective designs. Such design methodology is termed performance-based seismic design (PBSD) that is rapidly becoming widely accepted in professional practice. Using PBSD, structures can be designed to particular damage levels for different earthquake ground motions. PBSD formulated in the context of a structural optimization problem is a topic of growing interest and significant research studies have been conducted in recent years, regarding for example steel structures [14-20], reinforced concrete structures [21] and bridge piers [22-25].

Performance-based design optimization of composite structures, on the other hand is not addressed duly in the literature. Yet, a few publications dealing with optimization of composite buildings [26-28] did not consider performance-based design philosophy. Recently, Papavasileiou et al. [29] presented a structural optimization framework for seismic design of composite frames with SRC columns and steel beams and optional steel bracings. Although they applied inter-story drift constraints (maximum 4% for the collapse prevention performance level) by performing a displacement-controlled nonlinear pushover analysis, however, their formulation of the design optimization problem is not in the framework of a complete PBSD methodology, as well.

In this paper, a computer-aided design framework is developed for the optimal performance-based seismic design of Composite Moment Resisting Frames (CMRFs) consisting of concrete-filled steel box sections for column members and rolled steel I-shaped cross-sections for beam elements. Concrete-filled columns are considered to be built-up steel box sections instead of standard rolled tubes. The proposed design optimization procedure is then used to design two structural frames to the intended seismic performance.

2. PERFORMANCE-BASED SEISMIC DESIGN OF BUILDING STRUCTURES

Performance-based seismic design is the modern conceptual approach to structural design, which is based on the principle that a structure should meet performance objectives for multiple seismic hazard levels, ranging from small magnitude earthquakes of a short return period, to more intensive events with long return periods. A performance objective is a combination of performance levels each linked to a specific hazard level.

2.1 Performance levels

The performance level can be specified limits on any response parameter such as stresses, strains, displacements, accelerations, damage states or the failure probability [30, 31]. Various definitions and specifications of performance levels are introduced in the literature. According to FEMA-350 [32], four building performance levels are defined as per Table 1. This table also presents the correlation of performance levels with damage states. The roof drift ratio (RDR) and inter-story drift ratio (ISDR) are global response parameters successfully used to quantify structural performance. Allowable RDR limits for IO, LS and CP performance levels are suggested as 0.7%, 2.5% and 5%, respectively [33]. ISDRs corresponding to IO and CP levels are given in FEMA-350 (for low-rise buildings: 1.25% and 6.1% respectively). Based on the results of analyses on the performance of composite structures obtained by Muhummud [10], acceptable LS performance under the DE

earthquake is obtained with maximum RDR and ISDR limits of 2% and 3%, respectively. Satisfactory CP performance under MCE earthquake is realized when the roof and inter-story drift ratios are limited to 4% and 5%, respectively. These maximum allowable values of drift ratio are summarized in Table 2.

Table 1: Performance levels and corresponding damage states

Performance level	Damage state	Suggested drift limits
Operational (OP)	Minor damage	0.2%
Immediate Occupancy (IO)	Moderate damage	0.7%
Life safety (LS)	Severe damage	2.5%
Collapse Prevention (CP)	Near collapse	5%

Table 2: Maximum allowable values of response parameters

Response parameters	Performance level	
	LS	CP
RDR	2%	4%
ISDR	3%	5%

2.2 Seismic hazard levels

Seismic hazard is generally specified as the probability of exceedance of a certain hazard level or alternatively, the average return period for a given value of seismic hazard (e.g., ground acceleration or spectral acceleration). ATC-40 [34] specifies three levels of earthquake ground motion having 50%, 10% and 5% probability of exceedance in 50 years (mean return periods of approximately 75, 500 and 1000 years, respectively). These specified earthquake intensities are termed Serviceability earthquake, Design earthquake and Maximum earthquake respectively. FEMA-356 defines Maximum Considered Earthquake (MCE) hazard as a 2% probability of exceedance in 50 years (return period of approximately 2500 years). Based on these specifications, two levels of earthquake hazard are considered here for the design of composite moment frames, namely DE and MCE with 10% and 2% probability of exceedance in 50 years, respectively. The elastic spectral response acceleration for each hazard level may be obtained from the 5% damped spectral function as

$$S_a^i = \begin{cases} F_a^i S_s^i \left[0.4 + \frac{3T}{T_s^i} \right] & 0 \leq T \leq T_0^i \\ F_a^i S_s^i & T_0^i \leq T \leq T_s^i \qquad i = DE, MCE \\ \frac{F_v^i S_1^i}{T} & T_s^i \leq T \end{cases} \tag{1}$$

where T is the elastic fundamental period of the structure computed from structural analysis. S_s^i and S_1^i are mapped short-period response acceleration parameter and mapped response acceleration parameter at one-second period, respectively for each hazard level i. F_a^i and F_v^i are site coefficients and $T_0^i = 0.2T_s^i$ and $T_s^i = S_1^i/S_s^i$.

2.3 Performance objectives

The Basic Safety Objective is defined as achieving the LS performance level for a 10% in 50-year hazard level and the CP performance level for a 2% in 50-year earthquake.

3. MODELING AND ANALYSIS PROCEDURE

3.1 Modeling of structural components

Fiber model developed by Varma [2] for square CFT beam-column elements is used for modeling composite concrete-filled columns. The model is based on a distributed plasticity model where its nonlinear inelastic response is distributed along its length and cross-section. The concrete-filled steel box cross-section is discretized into concrete fibers and steel plate fibers as shown in Fig. 1. Monotonic stress-strain (σ−ε) curves for unconfined concrete, confined concrete and steel fibers are plotted in Fig. 2.

Beam members are simulated using simple lumped plastic hinges assigned to the ends of the elements. Nonlinear characteristics of the deformation controlled hinges are obtained from the material and geometric properties of the corresponding element cross-section.

3.2 Nonlinear Analysis procedure

A load-control pushover analysis (so called spectrum-based analysis in the literature [35]) is adopted for performance-based seismic design of CMRFs. In this method, the analysis is terminated when the maximum specified design base shear is achieved. The design base shear for a specified earthquake hazard level is determined using a site specific design spectrum. The method is an adaptive analysis in that the applied load pattern and the load increments continually change depending on the instantaneous dynamic characteristics of the system. Similar to the linear response-spectrum analysis method the load pattern in this pushover method can consider as many modes as deemed important during the course of the analysis. Hence, the effect of higher modes can be incorporated in the analysis and design.
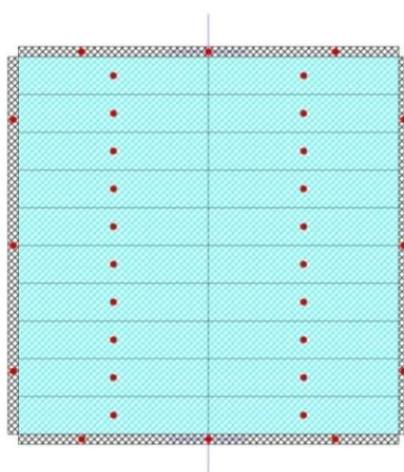

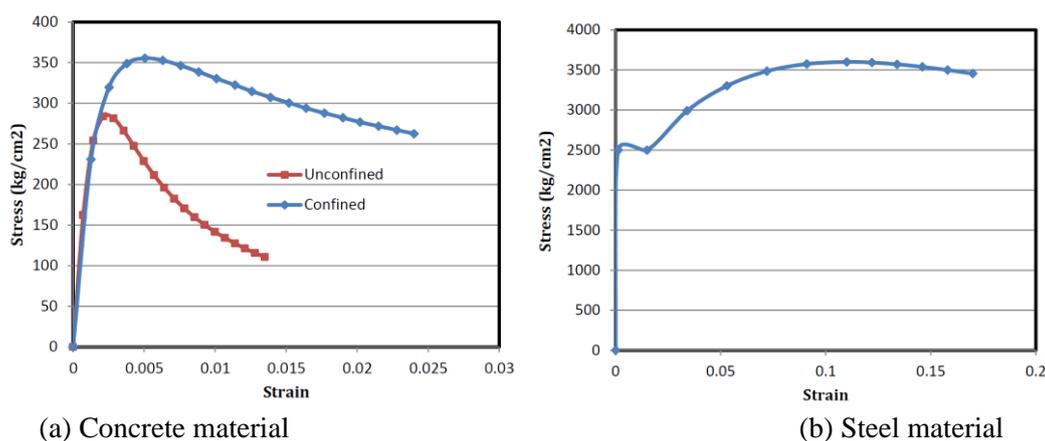Figure 1. Fiber element discretization of concrete-filled steel box cross-section

(a) Concrete material   (b) Steel material

Figure 2. Material properties

4. FORMULATION OF STRUCTURAL DESIGN OPTIMIZATION PROBLEM

4.1 Objective functions

Minimizing the Construction Cost is the primary objective of many structural optimization algorithms. However, in the context of performance-based design, minimum seismic damage under earthquake loading is an equally favorable objective. In this study, two objective functions concerning construction cost and seismic damage are explicitly incorporated into design.

Construction cost is considered proportional to the materials cost of the structural members i.e. steel-concrete columns and steel beams. Total material costs of a composite CFT composite structure is denoted by

$$C_{total} = C_s.M_s + C_c.V_c \qquad (2)$$

where C_s ($ per ton) and (Cc $ per m³) are the average total unit costs for steel and concrete, respectively. M_s and V_c are the total steel mass and concrete volume, respectively. By introducing the cost ratio CR (unite cost of concrete over unit cost of steel), the total cost can be replaced by the equivalent steel mass $M_{s(total)} = M_s + CR.V_c$. To facilitate the optimization process, $M_{s(total)}$ is normalized by dividing it by the maximum available total equivalent steel mass $M_{s(max)}$, which is obtained as the equivalent steel mass by selecting the upper-bound sections for all structural members. The cost function f_1 is then obtained as

$$f_1 = \frac{1}{M_{s(max)}}(M_s + CR.V_c) \qquad (3)$$

Another important objective in performance-based design concerns minimizing earthquake damage. Damage is quantified by relating it to inter-story drift distribution at extreme performance levels, such as CP level. Since uniform ductility demand over all stories generally avoids local weak-story collapse, minimum damage objective is interpreted

as providing a uniform inter-story drift distribution over the height of the building. To facilitate the structural optimization process, the uniform ductility objective function f_2 is formulated as a uniform story drift distribution normalized by the number of stories, ns:

$$f_2 = \left(\frac{1}{ns} \sum_{s=1}^{ns-1} \left(\frac{\theta_s}{\theta} - 1 \right)^2 \right)^{1/2} \qquad (4)$$

where θ_s and θ are the drift ratios at story s and roof level, respectively. In fact, equation 3 formulates the coefficient of variation of story drift ratio along the structure height. Minimizing f_2 under the MCE earthquake ensures a uniform distribution of damage and hence a minimum seismic damage at CP performance level.

4.2 Design Variables

Design variables are the section sizes to be selected from a set of discrete options. Two databases are provided: (a) square box sections for columns and (b) IPE sections for beams. Square box dimensions range from 160 to 600 mm with 10 mm increments. Minimum thickness is taken to be 2 mm and thickness values increase in 1 mm increments. AISC limitation on the maximum permitted width-to-thickness ratio ($5\sqrt{E/F_y}$) is also taken into account in selecting the feasible thickness values. Beams are selected from the set of standard rolled steel cross-sections ranging from IPE 120 to IPE 600. It is noted that no design variable is required to control the amount of concrete, since it is automatically determined by the steel box dimensions.

4.3 Design Constraints

4.3.1 Drift constraints
The overall building drift (roof drift) and inter-story drift are constrained under different earthquake hazard levels in order to ascertain the desired performance levels. As noted in section 2.1, roof drift ratio is limited to 2% and 4% under the DE and MCE earthquake hazard levels, respectively. The maximum allowable inter-story drift ratio is set to 3% and 5% under DE and MCE earthquakes, respectively. These limits are quantitative measures to ensure LS and CP performance under the respective DE and MCE seismic hazard levels. Although a uniform inter-story drift distribution was imposed at CP performance level through the objective function f_2, however provision of the above mentioned drift constraints further implies a uniform inter-story drift at less critical performance levels such as LS level.

4.3.2 Strength constraints
Under the action of seismic loads, member designs are usually governed by the drift constraints. However, the strength requirements should also be controlled in accordance with the design code provisions. As each member has several strength constraints for different load combinations, the number of such constraints for the entire structure would be very excessive. Therefore, direct implementation of strength constraints is faced with technical difficulties due to the enormous computational effort required. Recognizing this computational overburden and the additional fact that most of the strength constraints are

far from being active, an alternative approach is taken to implicitly account for member strength constraints. In this regard, a strength design is performed in each design cycle involving drift constraints, in accordance with the provisions of the governing design code (AISC-360 [36] herein). Member sizes obtained from the strength-based design are taken as the lower-size bounds on the design variables. In this way, the design optimization explicitly accounts for lateral drift constraints while implicitly accounting for the member strength requirements.

4.3.3 Strong column/weak beam (SC/WB) constraint

SC/WB concept is advocated in seismic provisions as a means to achieve higher levels of safety and energy dissipation by avoiding soft story mechanism. In this design philosophy, columns are designed strong enough such that flexural yielding generally takes place in beams, leaving the columns virtually free from the formation of plastic hinges except at the base of ground floor columns. The SC/WB requirement is implemented through the following constraint applied at beam-to-column connections [37]:

$$\frac{\sum M_{cnc}}{\sum M_{bpc}} > 1.1 \tag{5}$$

where, $\sum M_{cnc}$ is the sum of the moment capacities of the columns above and below the joint and $\sum M_{bpc}$ is the sum of the moment demands of the beams at the joint. A ten percent increase is introduced to recognize the potential over-strength of beams due to other unforeseen considerations. The optimization algorithm accounts for SC/WB constraints implicitly by applying the equation (5) at the strength design of moment-frames.

4.4 Optimization algorithm

The design optimization formulation includes two distinct objective functions namely the minimum structural weight (cost) and the minimum structural damage (uniform ductility distribution). Such a design problem is called multi-objective optimization. Evolutionary algorithms are most suited for solving multi-objective problems due to their population-based search method which allows to find an entire set of Pareto optimal solutions in a single run of the algorithm. Evolutionary optimization algorithms are now well established and successfully applied to different structural optimization problems, as discussed by Kaveh [38, 39]. A number of such algorithms which are developed and elaborated in recent years include Particle swarm optimization (PSO) [40], Ant colony optimization (ACO) [41], Big bang-big crunch (BB-BC) [42], Charged system search (CSS) [43], Ray optimization (RO) [44], Dolphin echolocation (DE) [45], Colliding Bodies Optimization (CBO) [46]. Each of these methods has its own advantages and shortcomings when applied to a particular type of optimization problem. A modified version of CBO algorithm denoted by MCBO is utilized in this paper to solve the optimization problem for performance-based seismic design of CMRFs. This method was recently applied to the optimization of post-tensioned concrete bridge superstructures [47], tunnel support linings [48] and performance-based seismic design of quasi-isolated bridge systems [25] and has shown to be of superior performance and easy to implement. The details of the algorithm and its computer implementation are elaborated in these references and are not restated here for the sake of brevity.

A number of techniques have been developed to deal with the multi-criteria optimization efficiently. Among the different approaches the so-called ε-constraint method is employed here due to its consistency with the objective functions employed for the current problem and the simplicity of the method for implementation. The method is based on minimization of the most preferred objective function (here the cost function), while the other objectives (here the uniform ductility objective) are considered as constraints bound by some allowable levels ε. Since the optimal value of the objective function f_2 is known (0 for the extreme case of a perfectly uniform inter-story drift distribution), this objective is implemented as a constraint with small bound value ε (0.05 for example). In fact, f_2 is thought as the coefficient of variation of the lateral translation distribution as mentioned in section 4.1.

4.5 Overall design procedure

The overall design procedure is illustrated by the flowchart in Fig 3.

5. NUMERICAL EXAMPLES

5.1 Example-1: Three-story frame

Consider the three-story, three-span moment frame in Fig. 4. The frame has rigid moment connections, with all column bases fixed at ground level. Based on the tributary areas, the seismic weights are taken as 120 ton for each story. The design variables consist of 3 types of column sections (C1 to C3) and 3 types of beam sections (B1 to B3). The column sections are chosen from among square boxes ranging in dimensions from 160 to 600 mm with 10 mm increments. Minimum plate thickness is taken to be 2 mm and thickness values increase in 1 mm increments up to the highest available thickness, which is assumed to be 50 mm. Nomenclature CFBXXXtXX is used to identify the concrete-filled box column sections, where the first three-digits indicate the box dimensions in mm and the second two-digits present the plate thickness. Beams are selected from the set of standard rolled steel cross-sections ranging from IPE-120 to IPE-600. As mentioned before, no design variable is required for the amount of concrete poured into the steel box cross-section. The value of cost ratio is estimated as CR = 0.03 ton/m3, which indicates a 'cheap' concrete and 'expensive' steel (The cost of one ton of steel is approximately 33.3 times the cost of one cubic meter of concrete). The corresponding upper bound sections (CFB600t50 for all columns and IPE-600 for all beams) are used to calculate the total maximum equivalent steel mass as $M_{s(max)}$=71.78 ton, which in turn is used to normalize the cost function f_1. The uniform ductility objective function f_2 is implemented using the ε-constraint technique with small bound value ε=0.05. Material strengths are assumed as f_y=2400 kg/cm^2 for steel yield strength and f_c=250 kg/cm^2 for concrete compressive strength. Site parameters for constructing the elastic response acceleration spectra at different seismic hazard levels are given in Table 3.
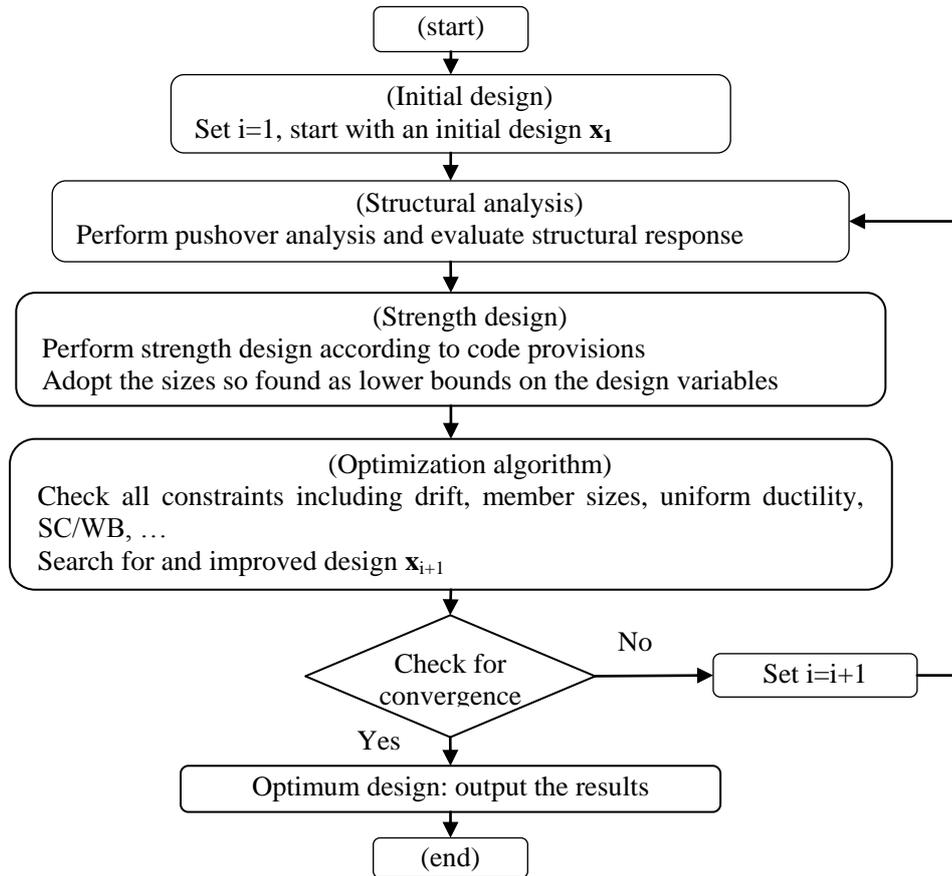
Figure 3. Flowchart of the proposed design optimization algorithm

The results of the performance-based seismic design optimization procedure are summarized in Table 4. The optimal value of the cost objective function is obtained as 0.0828 (i.e., the optimal equivalent steel mass of the frame is 0.0828×71.78=5.943 ton).

Table 3: Site parameters for design examples

Performance level	Earthquake hazard level	$S_s(g)$	$S_1(g)$	F_a	F_v
LS	DE	0.45	0.31	1.44	1.78
CP	MCE	0.7	0.45	1.24	1.55

Table 4: Design optimization results for Example-1

Design variable	C1	C2	C3	B1	B2	B3
Optimization results	CFB250t08	CFB250t06	CFB250t05	IPE-300	IPE-270	IPE-240
Equivalent total structural mass ratio (f_1)			0.0828			

The normalized base shear – roof drift ratio relationship (pushover curve) for the final design of the frame is plotted in Fig. 5. The two performance levels LS and CP under the corresponding DE and MCE earthquakes are also indicated in the plot. It is observed that for each performance level, the associated base shear is achieved at the maximum allowable roof drift ratio for that level i.e. 2% and 4% for LS and CP performance levels, respectively. This implies that the final design obtained by the optimization algorithm provides acceptable ductility capacity against the imposed earthquake demands.

Deformed shape of the frame at the corresponding LS and CP performance levels are shown in Fig 6, demonstrating the plastic hinge formation at beams and columns. It is observed from the figure that plastic hinges are confined to the beams and individual columns do not yield except at the base of the ground level columns. It can be argued that the application of SC/WB constraints results in a design which most likely eliminates any weak or soft story collapse mechanism. Also shown in this figure are the height-wise distribution of inter-story drift ratio. Fig. 6(b) indicates a nearly uniform distribution of inter-story drift at the CP performance level, as expected.

5.2 Example 2- Nine-story frame

Consider the nine-story, three-span moment frame in Fig. 7. Seismic weight of each story is calculated as 180 ton based on the tributary area. The design variables are reduced to 18, by grouping the columns and beams of each story i into section types Ci and Bi, respectively. The material strength, material cost ratio, design spectral parameters and allowable drift limits are taken to be the same as those of example 1. Total maximum equivalent steel mass of the frame used to normalize the cost function is calculated as $M_{s(max)} = 131.933$ ton.

The results of the performance-based design optimization procedure are summarized in Table 5. The optimal value of the cost objective function is obtained as 0.1575 (i.e., the optimal equivalent steel mass of the frame is $0.1575 \times 131.93 = 20.779$ ton)
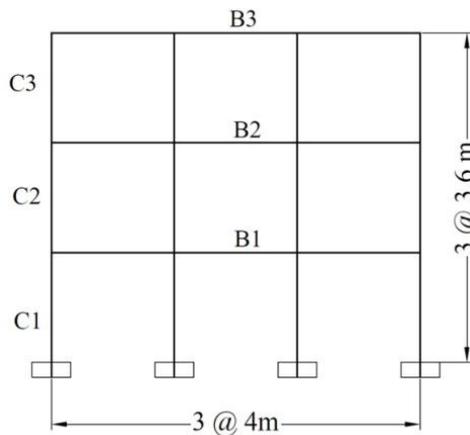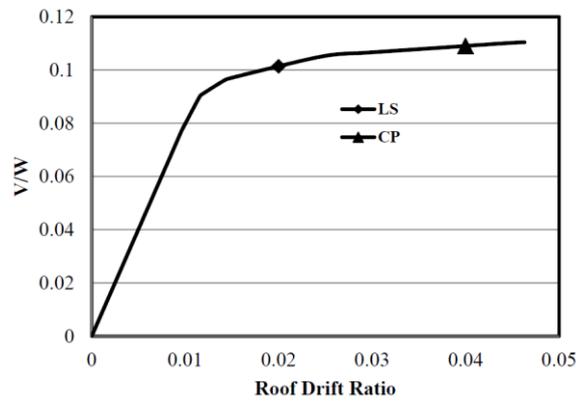

Figure 4. Three-story frame of Example-1
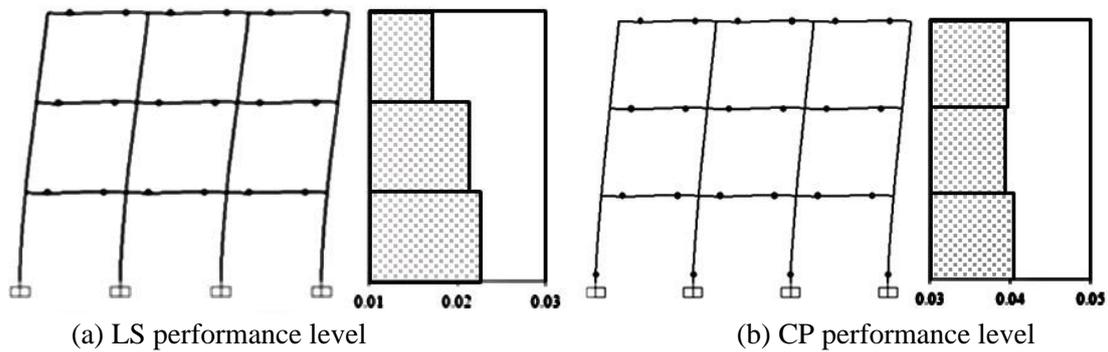
Figure 5. Pushover curve for Example-1

(a) LS performance level   (b) CP performance level

Figure 6. Three-story frame response (plastic state and inter-story drift ratio)

Table 5: Design optimization results for Example-2

Design variable (Column)	C1	C2	C3	C4	C5	C6	C7	C8	C9
Optimization results	CFB3 50t15	CFB3 50t12	CFB3 50t10	CFB3 50t08	CFB3 00t12	CFB3 00t10	CFB3 00t08	CFB2 50t08	CFB25 0t06
Design variable (Beam)	B1	B2	B3	B4	B5	B6	B7	B8	B9
Optimization results	IPE-400	IPE-400	IPE-360	IPE-360	IPE-330	IPE-330	IPE-300	IPE-270	IPE-240
Equivalent total structural mass ratio (f_1)	0.1575								

Fig. 8 presents the normalized pushover curve obtained for the final design of the frame. The two performance levels are also indicated in the plot. It is observed that the base shear demands at various performance levels are achieved at the maximum allowed roof drifts, indicating that the optimum design provides adequate ductility capacity.

Fig. 9 present plastic states of the frame at the corresponding LS and CP performance levels as well as the height-wise distribution of inter-story drift ratios. As noted in Example 1, the application of SC/WB constraints results in a frame design in which plasticity is confined to beam members and column yielding takes place only at the ground level. Such a

yielding mechanism is more favorable since the risk of a weak or soft story collapse is eliminated. Referring to Fig. 9 it noted that a nearly uniform distribution of inter-story drift at the CP performance level is obtained, indicating a uniform damage distribution along the stories.
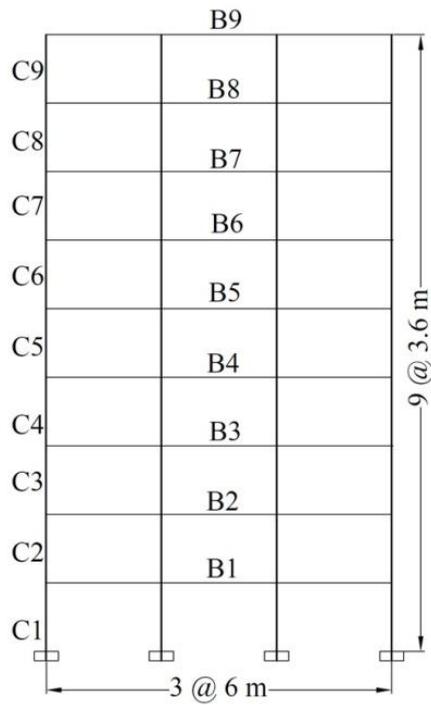

Figure 7. Nine-story frame of Example-2
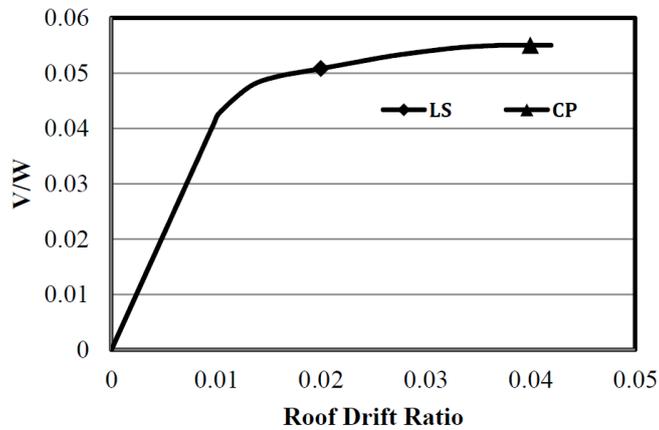

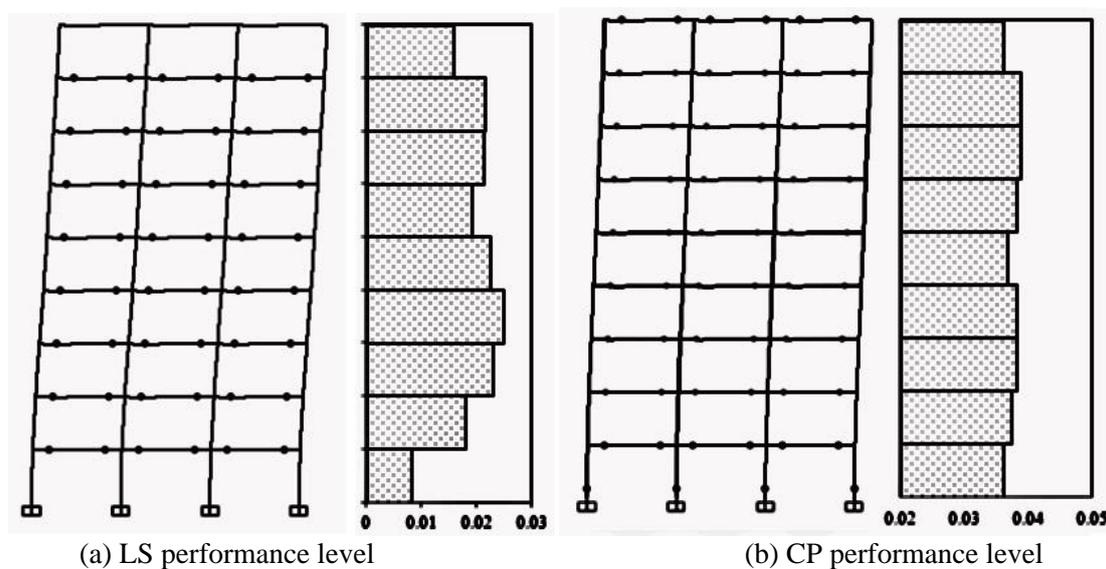Figure 8. Pushover curve for Example-2

<div align="center">

(a) LS performance level   (b) CP performance level

Figure 9. Nine-story frame response (plastic state and inter-story drift ratio)

</div>

6. CONCLUSION

A computer-aided design optimization procedure was developed for performance based seismic design of composite steel-concrete moment frames composed of concrete-filled steel box columns and bare steel beams. Two performance levels and corresponding earthquake intensities were considered. Cost and damage were taken as the two objectives to be minimized by the optimization algorithm. The multi-objective optimization problem was formulated and solved by integrating a load-control pushover analysis, a discrete evolutionary search method (MCBO algorithm) and the ε-constraint technique.

Two low- and mid-rise moment frames were presented as design examples. The obtained results show that the proposed design optimization approach is capable of producing seismic designs of composite moment frames which are cost effective, provide reliable seismic performance and suffer less damage in the case of a severe earthquake. Although the application of SC/WB constraints together with the uniform story drift distribution result in relatively heavier structures, however the optimum designs obtained consequently have a more reliable seismic performance due to the elimination of any weak or soft story collapse mechanism.

<div align="center">

REFERENCES

</div>

1. Tomii M, Sakino K. Experimental studies on the ultimate moment of concrete filled square steel tubular beam-columns, *Transact Architect Institute Japan* 1979; **275**: 55-65.
2. Varma AH, Ricles J, Sause R. Seismic behavior, analysis, and design of high strength square concrete filled steel tube (CFT) columns, Lehigh University, 2000.
3. Ricles J, Peng S, Lu L. Seismic behavior of composite concrete filled steel tube column-wide flange beam moment connections, *J Struct Eng* 2004; **130**(2): 223-32.

4. Roeder CW, Lehman DE, Bishop E. Strength and stiffness of circular concrete-filled tubes, *J Struct Eng* 2010; **136**(12): 1545-53.
5. Chen Z, Qin Y, Wang X. Development of connections to concrete-filled rectangular tubular columns, *Adv Steel Construct* 2014.
6. Choi SM, Park SH, Yun YS, Kim JH. A study on the seismic performance of concrete-filled square steel tube column-to-beam connections reinforced with asymmetric lower diaphragms, *J Construct Steel Res* 2010; **66**(7): 962-70.
7. Hajjar JF, Molodan A, Schiller PH. A distributed plasticity model for cyclic analysis of concrete-filled steel tube beam-columns and composite frames, *Eng Struct* 1998; **20**(4): 398-412.
8. Tort C, Hajjar JF. Mixed finite-element modeling of rectangular concrete-filled steel tube members and frames under static and dynamic loads, *J Struct Eng* 2010; **136**(6): 654-64.
9. Denavit MD, Hajjar JF. Nonlinear seismic analysis of circular concrete-filled steel tube members and frames, *J Struct Eng* 2011; **138** (9): 1089-98.
10. Muhummud T. Seismic behavior and design of composite SMRFs with concrete filled steel tubular columns and steel wide flange beams, Lehigh University, 2003.
11. Huang Z. Seismic behavior of moment resisting frames with high-strength square CFT columns, Michigan State University, 2005.
12. Denavit MD, Hajjar JF, Perea T, Leon RT. Seismic performance factors for moment frames with steel-concrete composite columns and steel beams, *Earthq Eng Struct Dyn*, 2016.
13. Hu JW, Kang YS, Choi DH, Park T. Seismic design, performance, and behavior of composite-moment frames with steel beam-to-concrete filled tube column connections, *Int J Steel Struct* 2010; **10**(2): 177-91.
14. Gholizadeh S, Kamyab R, Dadashi H. Performance-based design optimization of steel moment frames, *Int J Optim Civil Eng* 2013; **3**: 327-43.
15. Fragiadakis M, Lagaros ND, Papadrakakis M. Performance-based multiobjective optimum design of steel structures considering life-cycle cost, *Struct Multidisc Optim* 2006; **32**(1): 1-11.
16. Kaveh A, Azar BF, Hadidi A, Sorochi FR, Talatahari S. Performance-based seismic design of steel frames using ant colony optimization, *J Construct Steel Res* 2010; **66**(4): 566-74.
17. Kaveh A, Laknejadi K, Alinejad B. Performance-based multi-objective optimization of large steel structures, *Acta Mech* 2012; **223**(2): 355-69.
18. Gong Y. Performance-based design of steel building frameworks under seismic loading, University of Waterloo, 2004.
19. Fragiadakis M, Papadrakakis M. Performance-based optimum seismic design of reinforced concrete structures, *Earthq Eng Struct Dyn* 2008; **37**(6): 825-44.
20. Ataei H, Mamaghani M, Lui E. Proposed framework for the performance-based seismic design of highway bridges, *Structures Congress* 2017, pp. 240-53.
21. Kowalsky MJ, Priestley M, Macrae GA. Displacement-based design of RC bridge columns in seismic regions, *Earthq Eng Struct Dyn* 1995; **24**(12): 1623-43.
22. Sung YC, Su CK. Fuzzy genetic optimization on performance-based seismic design of reinforced concrete bridge piers with single-column type, *Optim Eng* 2010; **11**(3): 471-96.

23. Fazli H, Pakbaz A. Performance-based seismic design optimization for multi-column RC bridge piers, considering quasi-isolation, *Int J Optim Civil Eng*, 2018; **8**(4): 525-45.

24. Chan CM. Optimal lateral stiffness design of tall buildings of mixed steel and concrete construction, *Struct Des Tall Build* 2001; **10**(3): 155-77.

25. Cheng L, Chan CM. Optimal lateral stiffness design of composite steel and concrete tall frameworks, *Eng Struct* 2009; **31**(2): 523-33.

26. Lagaros ND, Magoula E. Life-cycle cost assessment of mid-rise and high-rise steel and steel–reinforced concrete composite minimum cost building designs, *Struct Des Tall Special Build* 2013; **22**(12): 954-74.

27. Papavasileiou GS, Charmpis DC. Seismic design optimization of multi-storey steel-concrete composite buildings, *Comput Struct* 2016; **170**: 49-61.

28. Ghobarah A. Performance-based design in earthquake engineering: state of development, *Eng Struct* 2001; **23**(8): 878-84.

29. Poland CD, Hill J, Sharpe RL, Soulages J. Vision 2000: Performance Based Seismic Engineering of Buildings. Structural Engineers Association of California (SEAOC), 1995.

30. Federal Emergency Management Agency. Recommended Seismic Design Criteria for New Steel Moment-frame Buildings: FEMA-350: SAC Joint Venture, 2013.

31. Federal Emergency Management Agency. NEHRP Guidelines for the seismic rehabilitation of buildings: FEMA-273. Federal Emergency Management Agency Washington, DC, 1997.

32. Applied Technology Council. Seismic evaluation and retrofit of existing concrete buildings: ATC-40. Redwood City (CA), 1996.

33. Gupta B, Kunnath SK. Adaptive spectra-based pushover procedure for seismic evaluation of structures, *Earthq Spectra* 2000; **16**(2): 367-92.

34. American Institute of Steel Construction. ANSI/AISC 360, Specification for Structural Steel Buildings, Chicago, Illinois 2010.

35. American Institute of Steel Construction. ANSI/AISC 341, Seismic Provisions for Structural Steel Buildings, Chicago, Illinois 2002.

36. Kaveh A. *Advances in Metaheuristic Algorithms for Optimal Design of Structures*, Switzerland, Springer International Publishing, 2017.

37. Kaveh A. *Applications of Metaheuristic Optimization Algorithms in Civil Engineering*, Switzerland, Springer, 2017.

38. Eberhart RC, Kennedy J. A new optimizer using particle swarm theory, *Proceedings of the Sixth International Symposium on Micro Machine and Human Science* 1995, New York, NY, pp. 39-43.

39. Dorigo M, Maniezzo V, Colorni A. Ant system: optimization by a colony of cooperating agents, *IEEE Transact Syst, Man, Cybernet, Part B (Cybernet)* 1996; **26**(1): 29-41.

40. Erol OK, Eksin I. A new optimization method: big bang–big crunch, *Adv Eng Softw* 2006; **37**(2): 106-11.

41. Kaveh A, Talatahari S. A novel heuristic optimization method: charged system search, *Acta Mech* 2010; **213**(3-4): 267-89.

42. Kaveh A, Khayatazad M. A new meta-heuristic method: ray optimization, *Comput Struct* 2012; **112**: 283-94.

43. Kaveh A, Farhoudi N. A new optimization method: Dolphin echolocation, *Adv Eng Softw* 2013; **59**: 53-70.
44. Kaveh A, Mahdavi V. Colliding bodies optimization: a novel meta-heuristic method, *Comput Struct* 2014; **139**: 18-27.
45. Kaveh A, Maniat M, Naeini MA. Cost optimum design of post-tensioned concrete bridges using a modified colliding bodies optimization algorithm, *Adv Eng Softw* 2016; **98**: 12-22.
46. Fazli H. Optimal design of tunnel support lining using mcbo algorithm, *Int J Optim Civil Eng* 2017; **7**(3): 339-54.